Large and ultrafast photoinduced reflectivity change in the charge separated phase of $Et_2Me_2Sb[Pd(1,3\text{-dithiol-}2\text{-thione-}4,5\text{-dithiolate})_2]_2$

T. Ishikawa,[1] N. Fukazawa,[1] Y. Matsubara,[1] R. Nakajima,[1] K. Onda,[1] Y. Okimoto,[1] S. Koshihara,[1,2] M. Lorenc,[3] E. Collet,[3] M. Tamura,[4,*] and R. Kato[4]

[1]*Department of Materials Science, Tokyo Institute of Technology, 2-12-1 Oh-Okayama, Meguro, Tokyo 152-8551, Japan*

[2]*Nonequilibrium Dynamics Project, ERATO-JST, Tsukuba, Ibaraki 305-0801, Japan*

[3]*Institut de Physique de Rennes, UMR 6251, CNRS–Université de Rennes 1, 35042 Rennes Cedex, France*

[4]*RIKEN, 2-1 Hirosawa, Wako, Saitama 351-0198, Japan*

(Received 8 December 2008; revised manuscript received 16 June 2009; published 9 September 2009)

A large photoinduced change in reflectivity has been observed in the low-temperature charge separated (CS) phase of a dimeric radical anion salt, $Et_2Me_2Sb[Pd(dmit)_2]_2$ (dmit=1,3-dithiol-2-thione-4,5-dithiolate). Just after the photoexcitation, the reflectivity abruptly changed reflecting the appearance of a photoinduced metastable state, indicating occurrence of recrystallizing of the CS phase by intradimer photoexcitation within a picosecond. Quantitative analysis considering the linear combination of the dielectric functions of the CS and the dimer-Mott state suggests a rather high efficiency of the photoinduced phase transition. One photon can change the valence of about five dimers. This photoinduced metastable state relaxed to the initial CS state via two successive types of relaxation processes, a fast and a slow one. The relaxation time (τ) and the reflectivity of the fast process showed a clear excitation intensity and temperature dependence. In particular, τ and the estimated domain size were enhanced up to the transition temperature (T_c) with increasing temperature. This phenomenon, a sort of critical slowing down around T_c, suggests that the density of the photoinduced state as well as the external temperature plays an important role in determining the relaxation dynamics of the photoinduced state. The results obtained indicate that this photoinduced phenomenon can be classified as a tuning of the charge in crystals via cooperative interaction between the degrees of freedom of "charge" and "molecular orbital" of the constituents, i.e., as a type of photoinduced phase transition.

DOI: 10.1103/PhysRevB.80.115108 PACS number(s): 78.47.J−, 82.53.Xa, 33.20.Ea, 71.30.+h

I. INTRODUCTION

In recent developments in materials science, the search for crystals with highly efficient and ultrafast photoresponse, so-called photoswitching materials, has occupied an important place in both fundamental and applied studies. The idea of photoinduced phase transition (PIPT) phenomena has become an important target of extensive research as a basic and attractive concept for designing materials with a highly photosensitive response and photoswitchable properties.[1–4] An enhanced photoresponse can be expected by the cooperative interaction among constituent molecules in the dynamical processes of PIPT phenomena.

In molecular crystals, the lattice and structure of constituent molecules are generally considered to be strongly coupled to the electronic state by virtue of the flexibility of the crystal. In other words, the "molecular orbital" degrees of freedom of each constituent will interfere with the electronic state of the whole crystal via electron-lattice interactions. In addition, the molecules are weakly bonded together and consequently, the molecular crystals have rather narrow bandwidths compared to inorganic compounds. It is to be naturally expected that strong electron-lattice interaction and strong electron-electron correlation due to the small bandwidth compete/cooperate with each other in molecular crystals, and become the origin of multistability in the potential energy. Such a condition is an important merit for designing PIPT systems, and indeed various PIPT phenomena have been observed in this class of organic materials.[1,2,4–8] Among them, charge-ordering (CO) systems occupy an important position, because they show real space alignment of the charge strongly coupled with the deformation of lattice and constituent molecules, and thus are very sensitive to charge transfer type photoexcitation.[2,4,5,7,8] It is a natural idea that melting of CO triggered by photoexcitation induces insulator-to-metal transitions in this class of materials.[2,4,5,7,8]

Here, we report efficient and ultrafast photoinduced reflectivity change in a newly developed material, $Et_2Me_2Sb[Pd(dmit)_2]_2$ (dmit=1,3-dithiol-2-thione-4,5-dithiolate). This compound crystallizes in a layered structure, in which conducting anion layers made of $Pd(dmit)_2$ and insulating cation layers of Et_2Me_2Sb are alternately stacked. The crystal structure of the conduction layer at room temperature is schematically shown in Fig. 1(a). In the anion layer, $Pd(dmit)_2$ molecules are stacked face-to-face with changing directions from layer to layer (along the $\boldsymbol{a}+\boldsymbol{b}$ and $\boldsymbol{a}-\boldsymbol{b}$ axis) to form a solid-crossing structure. The formal charge of $Pd(dmit)_2$ is $-1/2$. However, the system has a half-filling character as a result of very strong dimerization.[9] Figures 2(a) and 2(b) show the temperature dependence of the resistivity along the $\boldsymbol{a}$ axis and the optical reflectivity (R) observed at a photon energy of 1.3 eV with the electric field parallel to the $\boldsymbol{a}$ axis, respectively. The resistivity is high and its temperature dependence shows insulating behavior reflecting the nature of a half-filled system; this high temperature phase is named the dimer-Mott (DM) phase.[10–12] As the temperature decreases, this crystal shows a unique phase transition at around $T_c=70$ K as shown in Figs. 2(a) and 2(b) with small hysteresis.[13,14] The resistivity increases more rapidly as the temperature decreases in this low-temperature

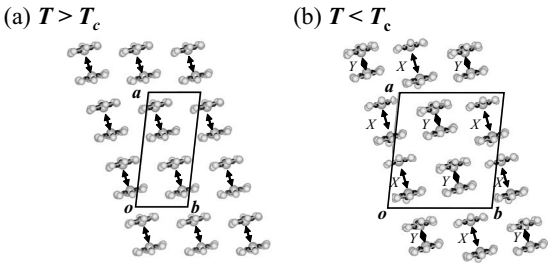

FIG. 1. Schematic structure of the anion layer of $Et_2Me_2Sb[Pd(dmit)_2]_2$ viewed along the long direction of the molecules. (a) End-on projection of the DM insulating phase, (b) that for the charge separated (CS) phase. *X* and *Y* denote two crystallographically independent dimers. *X* is an expanded divalent dimer and *Y* is a constricted neutral dimer. [15] Solid lines represent the end-on projection of the ***ab*** plane in the unit cell.

phase compared to the DM phase, which suggests a change in the gap energy. According to previous studies,[12,13,15,16] this material exhibits real space ordering of charges in this low-temperature phase. In other words, the valence of the dimers is not uniform and the two kinds of dimers, which have

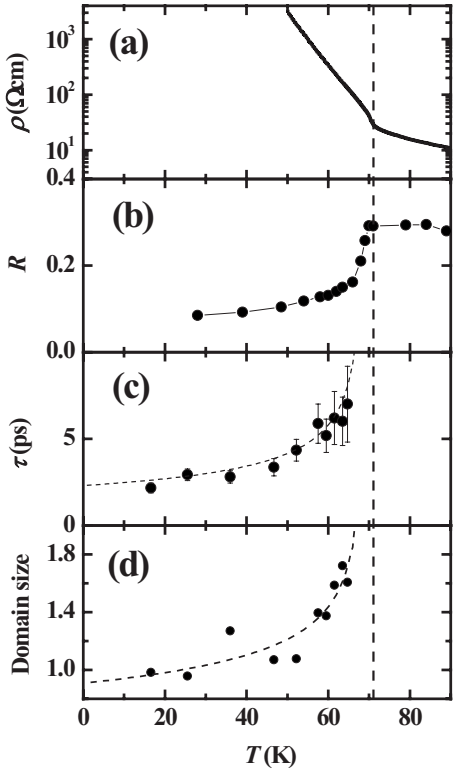

FIG. 2. Temperature dependence of (a) resistivity (ρ), (b) reflectivity observed at 1.31 eV (R), (c) the relaxation time (τ) estimated from the time profile of the photoinduced reflectivity change, and (d) the estimated relative photoinduced domain size at 0.5 ps (see context in Sec. VII), respectively. The pump photon energy for pump-probe measurements was 1.55 eV with an intensity of $1.18 \times 10^{20}/\mathrm{cm}^3$. For the probe light, the photon energy was 1.31 eV. The transition temperature is about 70 K judging from the kink of resistivity and reflectivity (indicated by dashed vertical line). The relative size of the photoinduced domain [in (d)] is normalized with that observed at 16.6 K.

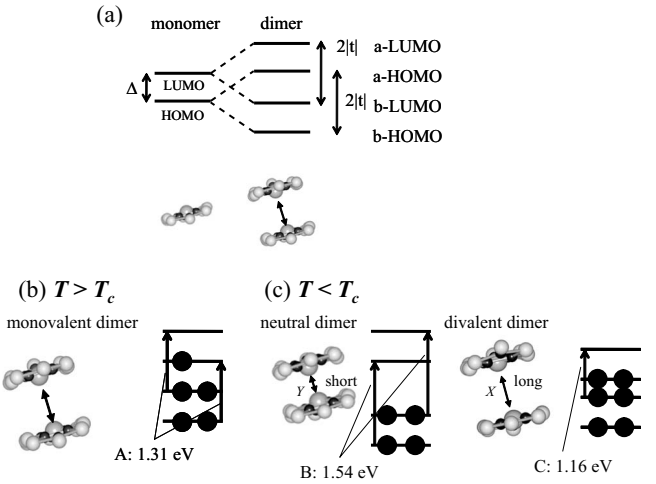

FIG. 3. (a) Schematic energy diagram of $Pd(dmit)_2$ monomer and dimer. Schematic shape of the $Pd(dmit)_2$ monomer and dimer are also drawn under the energy diagram. (b) Schematic structure of the monovalent (−1) $Pd(dmit)_2$ dimer and its energy level. (c) Those for the neutral (0) and divalent (−2) $Pd(dmit)_2$ dimers and their energy levels. Arrows drawn in (b) and (c) represent the intradimer transition observed in the optical reflectivity in the near-IR region (see Fig. 4 and Ref. 13). *A*, *B*, and *C* correspond to the peak structures in Fig. 4. The values of the energy between the bonding and antibonding state are quoted from Ref. 12.

different intermolecular spacing, are ordered as shown schematically in Fig. 1(b).[15]

Similar to CO materials, the charges are also coupled to the lattice deformation in $Et_2Me_2Sb[Pd(dmit)_2]_2$. However, in contrast, the microscopic mechanism involved is based on the unique nature of the multilevel electronic structure of the dimer, i.e., coupling between the degree of freedoms of the "molecular orbital" and "lattice structure."[12,13,15,16] Therefore, this unique phase transition should be clearly discriminated from the usual CO phenomena appearing in the nonhalf-filling cases, in which intersite Coulomb repulsion plays the main role.[17] This peculiar low-temperature phase reflecting the unique nature of the molecular orbital of the dimer ($[Pd(dmit)_2]_2$) has been named the "charge-separated" (CS) phase to distinguish it from conventional CO.[12,15] The obtained results and associated quantitative analysis strongly suggest the occurrence of a new class of PIPT from the CS to DM phase. In other words, Insulator-to-Insulator PIPT which is different from the conventional Insulator-to-Metal PIPT seems to be driven by femto second (fs)-pulsed laser light in this crystal. This indicates that the CS system provides a new class of candidate for the study of PIPT materials. We also show that the relaxation process of the photoinduced metastable state is closely related to both the excitation intensity and the temperature of the system.

Figures 3(a)–3(c) show the diagrams of the molecular energy level of the monomers and dimers in the high and low-temperature phases. As shown in Fig. 3(a), it is an important nature of the $Pd(dmit)_2$ dimer systems that the energy splitting between the lowest unoccupied molecular orbital (LUMO) and highest occupied molecular orbital (HOMO) states of the monomer (Δ) is rather small compared to the

large energy gain due to the dimerization ($|t|$).[16] Thus, there is an interchange in the energy level between the bonding state of the dimer consisting of LUMO of monomers (b-LUMO) and the antibonding state of the dimer consisting of the HOMO of monomers (a-HOMO), as schematically shown in Fig. 3(a).[13] It should be noted that among the four molecular orbitals of the dimer derived from HOMO and LUMO of monomers, the highest two are unstable due to their antibonding nature even though one of them originates from the HOMO of monomers. When these antibonding states are empty, the dimerization can be strong to stabilize the bonding states since the dimer has neutral charge and it is not affected by Coulomb repulsion between the monomers. Theoretical calculations have revealed that this neutral dimer can be largely stabilized due to strong dimerization.[13,16] This stabilization mechanism is the origin of the CS phase transition, as indicated in Figs. 3(b) and 3(c), in spite of the energy cost of generating an unstable divalent dimer with rather weak dimerization.[16] This mechanism is quite different from that for conventional CO systems, wherein long-range coulomb repulsion or the cooperative Jahn-Teller effect plays a key role for charge separation.[17]

This unique CS phase can be clearly identified by the reflectivity spectrum.[12] The reflectivity shows characteristic peak structures in the near-infrared (IR) range (solid lines in Fig. 4), which is assigned to the intradimer photoexcitation between b-HOMO and a-HOMO (or energetically equivalent photoexcitation between b-LUMO and a-LUMO) [indicated by upward arrows in Figs. 3(b) and 3(c)]. These peak energies directly reflect the degree of dimerization closely related to the valence of the dimers.[13,16] Peaks *A*, *B*, and *C* in Fig. 4(a) are the intradimer photoexcitation in the monovalent dimer, the neutral dimer, and the divalent dimer, respectively. This work was motivated by expectation that the photoexcitation of the intradimer optical band can trigger melting of the charge alignment, if the strong stability of the neutral dimer is the origin of the CS phase. This is the reason why the correlated molecular system with the CS phase is classified as an important target for the development of new PIPT materials. However, thus far, there have been almost no studies on this class of materials, except for the simple observation of a photoinduced spectral change in a rather narrow photon-energy region.[18] Here, we report photoinduced spectral changes in $Et_2Me_2Sb[Pd(dmit)_2]_2$ single crystals over a wide photon-energy region, which is essential for identifying the photoexcited state. In addition, we also demonstrate quantitative analysis of the dynamical behaviors of the photoexcited state based on the temperature dependence of fs time-resolved reflectivity spectra in detail.

II. EXPERIMENT

Single crystals of $Et_2Me_2Sb[Pd(dmit)_2]_2$ were obtained by an oxidation process of $[Et_2Me_2Sb]_2[Pd(dmit)_2]$ in air.[15] In order to confirm the transition temperature of the crystal, we performed two-probe resistivity and optical reflectivity measurements at various temperatures [Figs. 2(a) and 2(b)]. We also carried out pump-probe time-resolved reflection spectroscopy measurements. A fs-pulsed laser from a Ti:Sapphire regenerative amplifier (pulse width: 120 fs, photon energy: 1.58 eV, repetition rate 1 kHz, Quantronix Integra) was utilized as the light source. We can control the photon energy of the pump and probe light using the optical parametric amplifier (OPA, Light conversion TOPAS). The size of the spot of the pump light was adjusted to be around 350 μm diameter and that of the probe light was adjusted to within 50 μm diameter. The time delay between the pump and probe lights was controlled using the translational stage to create a difference in the optical path length. We used a photodiode-type photodetector in the study. In order to accumulate data with a good S/N ratio, we utilized a box-car-type integrator. The samples were fixed on a copper-based sample holder and loaded in a liquid He exchange type dynamic flow optical cryostat (Oxford Optistat) equipped with quartz windows for optical measurements.

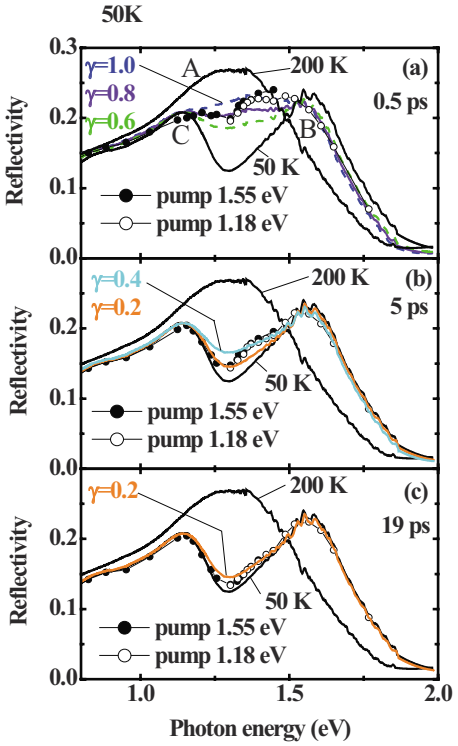

FIG. 4. (Color online) Closed and open circles represent the photoinduced reflectivity spectra ($\boldsymbol{E}\|\boldsymbol{a}$ axis) with excitation photon energy of 1.55 and 1.18 eV, respectively, at (a) 0.5, (b) 5, and (c) 19 ps after photoirradiation. The excitation intensity was $1.4\times10^{20}/cm^3$ at 1.55 eV pump and $7.6\times10^{19}/cm^3$ at 1.18 eV pump. Solid lines show the spectra without photoexcitation at 50 (CS phase) and 200 K (DM phase) in each figure. The colored solid lines and dashed lines show the simulated reflectivity spectra using the multilayer model with several photoconversion efficiency (see text). A, B, and C indicate the peak structures corresponding to Figs. 3(b) and 3(c).

III. GENERATION AND RELAXATION DYNAMICS OF THE PHOTOINDUCED STATE IN THE CS PHASE

Figure 5(a) shows typical data of the photoinduced reflectivity change induced by pulsed laser irradiation at 50 K (CS

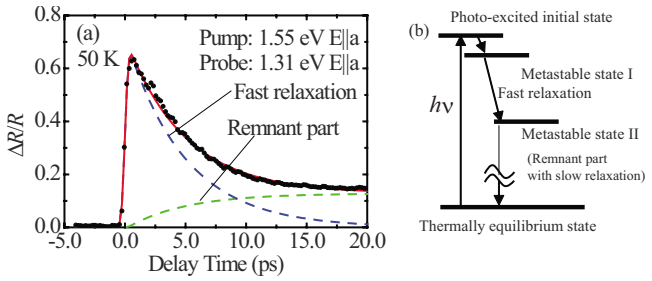

FIG. 5. (Color online) (a) Typical time profile of the pump-probe signal ($\Delta R/R$) with excitation of 1.55 eV light (closed circles). The probe photon energy was 1.31 eV. The dashed blue (gray), dashed green (light gray), and solid red (gray) curves represent fast relaxation, remnant part, and their summation, respectively (see context), estimated based on the fitting procedure. (b) Schematic energy diagram of the photoinduced relaxation processes.

phase). Here $\Delta R/R$ is defined as $\Delta R/R=[R(t)-R_0]/R_0$. $R(t)$ is the reflectivity at a delay time t. R_0 is the reflectivity without the pump light. For the pump light, the photon energy was 1.55 eV and the polarization was parallel to the ***a*** axis of the crystal. As shown in the reflectivity spectrum without excitation at 50 K (see solid line in Fig. 4), the pump photon energy corresponds to a near-IR peak on the higher energy side [peak B in Fig. 4(a)], which is assigned to intradimer photoexcitation in the neutral dimer [upward arrows in Fig. 3(c)].[13] The probe photon energy was set to 1.31 eV ($\boldsymbol{E}\|\boldsymbol{a}$ axis) at which the reflectivity shows a large spectral change accompanied by a thermal phase transition. Immediately after the photoexcitation, the reflectivity rapidly increased within about 0.5 ps to reach the peak values. Such a fast response implies that this photoinduced response has an electronic origin, and not a simple thermally induced one.[1] A gradual decrease in the photoresponse follows the peak in the time profile. To analyze the relaxation processes, we performed fitting analysis using the summation of exponential decay and a remnant part, $f(t)=A\exp\{-(t-t_0)/\tau\}+B[1-\exp\{-(t-t_0)/\tau\}]$. In addition, the response function of the measurement system is taken into account. The result is also plotted by the red (gray) solid line in Fig. 5(a) and it corresponds well with the observed result. The relaxation time of the photoresponse is closely related to the temperature and excitation intensity as discussed in Secs. VI and VII. Here it should be noted that there seem to be three processes in the photoinduced dynamics: (1) a rising edge just after the excitation corresponding to formation of a photoinduced metastable state I, (2) fast relaxation (exponential part shown as the dashed line), and (3) remnant part shown as the dotted line due to formation of a metastable state II. The schematic energy diagram of these relaxation processes is plotted in Fig. 5(b). Just after the photoexcitation, one $Pd(dmit)_2$ dimer should be the photoexcited initial state according to the Franck-Condon approximation. Such a photoexcited dimer induces the electronic structural change in the surrounding dimers resulting in a photoinduced metastable state (metastable state I) within the time-scale of the first rising edge, as discussed in Sec. V. This metastable state I shows a fast relaxation process and is transformed into metastable state II, which has a long relaxation time. The fast relaxation process of the photoinduced metastable state I will be discussed in Sec. VI.

IV. PUMP PHOTON-ENERGY DEPENDENCE OF THE PHOTOINDUCED RESPONSE

In this section, prior to the discussion on the metastable state I and its relaxation, the pump photon-energy dependence of the photoinduced signal will be first discussed, because a detailed study of photoinduced reflectivity changes over the wide photon-energy region can be accomplished only with data utilizing various excitation photon energies, as discussed below.

There are two kinds of intradimer photoexcitation processes in the CS phase corresponding to the existence of two types of dimers.[13] We have investigated the pump photon-energy dependence of the photoinduced reflectivity change. Typical results are shown in Fig. 6. Three typical data sets show little difference in the time profile of $\Delta R/R$ between excitations of 1.18 and 1.55 eV. This similarity suggests that the photoinduced metastable state in each excitation condition experiences similar relaxation processes; in other words, the metastable states generated during the relaxation process from the Franck-Condon state is common for both cases of 1.18 and 1.55 eV excitation photon energy, though we could select which kind of dimer was photoexcited. It seems to be a reasonable idea that the wave function of a-HOMO and a-LUMO of dimers are spread sufficiently to neighboring dimers, and the excited electron can easily move between dimers to form a metastable state within the time-scale of the rising edge.

During the time-region of the fast relaxation process, oscillatory components were clearly observed [see Figs. 6(a)–6(c)]. To analyze these oscillations, the oscillatory components were extracted using the subtraction of the nonoscillatory component, which can be reproduced by the above fitting procedure using the exponential relaxation functions [see Figs. 6(f) and 6(g)]. We then analyzed these components by the wavelet analysis procedure. The resulting contour maps are plotted in Figs. 6(h) and 6(i). In each case, the results show similar behavior again. This similarity supports the above idea that two different kinds of photoexcitation result in a common metastable state in the first stage of the photoinduced effect. Just after the photoexcitation, two oscillation modes that have significant amplitudes were observed clearly at around 20 and 50 cm^{-1}. During the fast relaxation process ($t<$ about 10 ps), the frequencies of these two modes change gradually and seem to merge into a single mode (around 25 cm^{-1}). At the present stage, we tentatively assign these coherent oscillation modes to the modulation of the intermolecular spacing in the $Pd(dmit)_2$ dimer since the observed photoinduced coherent oscillations have much lower frequency than the internal molecular oscillation. Such an oscillation is expected to have strong coupling with the change in the valence of the dimer. It should be noted that the change in the frequency occurs in a similar time-scale as the fast relaxation, and this parallel behavior strongly suggests that these two phenomena, electronic relaxation and lattice response, have the same origin.

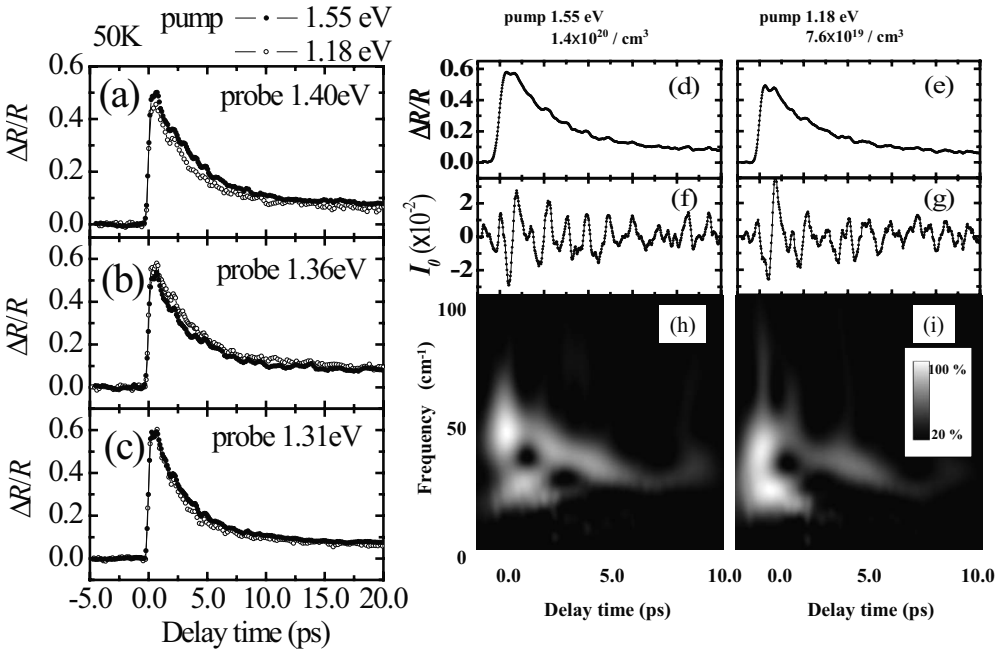

FIG. 6. (a), (b), and (c) Excitation photon-energy dependence of time profiles of the pump-probe signal ($\Delta R/R$) observed at three probe photon energies (1.31, 1.36, and 1.40 eV). The closed circles represent the signal for the pump photon energy of 1.55 eV with intensity of $1.4\times10^{20}/\mathrm{cm}^3$. The open circles represent the pump photon energy of 1.18 eV with intensity of $7.6\times10^{19}/\mathrm{cm}^3$. (d), (e) Time profiles of the pump-probe signal with different pump photon energies. (f), (g) Oscillatory components extracted by subtracting the electronic component (see text). (h), (i) Contour maps of the results of wavelet analysis of the oscillatory components. The inset in (i) shows the scale of these plots.

V. SPECTRA OF THE PHOTOINDUCED STATE

The electronic structure of the photoinduced state has been investigated using reflectivity spectra. We measured the reflectivity spectra of the photoinduced state in the energy scale of the intradimer photo excitations at several delay times, keeping the sample temperature at 50 K. The probe photon energy was swept between 0.8 and 2 eV to fully cover the photon energy of the whole part of the intradimer electron transition. The excitation photon energies were fixed at 1.55 eV and 1.18 eV. Two data sets of different excitation photon energies are summarized and plotted in Figs. 4(a)–4(c). It is a reasonable procedure to summarize two data sets for different excitation conditions and obtain the complete reflectivity spectra over a wide photon-energy region, as discussed in Sec. IV. Spectra obtained just 0.5, 5, and 19 ps after excitation are plotted, respectively, in Figs. 4(a)–4(c). The solid lines represent the reflectivity spectra at 50 K (CS phase) and the spectra at 200 K (DM phase) without photoexcitation. In this photon-energy region, the near-IR absorption peaks observed for light polarized along the ***a*** axis are due to intradimer photoexcitation between the bonding and antibonding states, as shown in Figs. 3(b) and 3(c), directly reflecting the degree of dimerization and the valence of the dimers.[12]

Just after the photoexcitation [Fig. 4(a)], the valley between the two near-IR peaks seems to be filled, whereas a small reflectance change was observed outside of the two peaks (i.e., below 1.2 eV and above 1.6 eV). Similar features are observed 5 and 19 ps after the photoirradiation. In order to understand the electronic origin of the ultrafast reflectance change, we performed detailed analysis of the data. We assumed a homogeneous state of the surface and considered that the dielectric function (ε) can be described by a linear combination of ε in the CS state and the initial state;[6,19]

$$\varepsilon(x) = \varepsilon^{\mathrm{HT}}\gamma\exp\left(-\frac{x}{d}\right) + \varepsilon^{\mathrm{LT}}\left\{1-\gamma\exp\left(-\frac{x}{d}\right)\right\}.$$

Here, x is the distance from the sample surface, $\varepsilon^{\mathrm{HT}}$ and $\varepsilon^{\mathrm{LT}}$ are ε at 200 and 50 K which can be attributed to the DM and CS phase, respectively (we assumed that the DM phase was a photoinduced state in this analysis), and γ is the yields of the observed PIPT ($0<\gamma<1$). The penetration depth of the pump light (1.55 eV), d, is about 50 nm, as estimated by Kramers-Kronig analysis using measured static optical reflectivity. From $\varepsilon(x)$, we exactly calculated the reflectivity spectra with several γ values as shown by the solid lines in Fig. 4. The calculated spectra reproduce these spectral features very well in the photoinduced reflectivity. Thus, these results indicate that the electronic structure of the photoinduced phase is the DM phase as assumed by us. The estimated γ value at 0.5 ps ($\gamma=0.8-1.0$) shows that one excitation photon converts about five dimers under the present excitation condition. Based on this result, we have depicted the above ultrafast features in Fig. 5(b). By way of the Franck-Condon state, the monovalent dimers, similar to the high temperature DM phase (Metastable state I), are generated within 1 ps with charge transfer between the divalent and neutral dimers.

At 5 and 19 ps after excitation, the change in reflectivity decreases gradually, as shown in Figs. 4(b) and 4(c), corre-

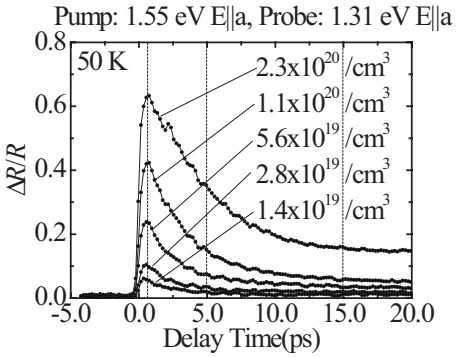

FIG. 7. (a) Excitation intensity dependence of the pump-probe signal $(\Delta R/R)$ of $Et_2Me_2Sb[Pd(dmit)_2]_2$ at 50 K. The polarization of the 1.55 eV pump and 1.31 eV probe lights was parallel to the ***a*** axis of the crystal. The photon densities of the pump light were 2.3×10^{20}, 1.1×10^{20}, 5.6×10^{19}, 2.8×10^{19}, and $1.4\times10^{19}/\mathrm{cm}^3$.

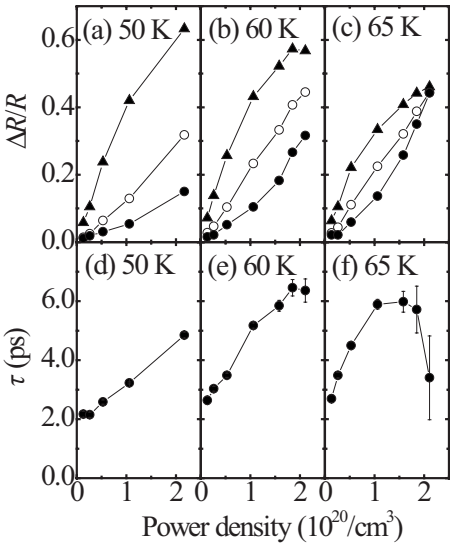

FIG. 8. (a), (b), (c) Excitation intensity dependence of the reflectivity change $(\Delta R/R)$ at 50, 60, and 65 K. Closed triangles, open circles, and closed circles show the data at 0.5, 5.0, and 15.0 ps after photoexcitation, respectively. (d), (e), (f) Excitation intensity dependence of the relaxation time of the fast relaxation (τ) with error bars at 50, 60, and 65 K, respectively.

sponding to the fast relaxation process (exponential part) observed in the time profile following the initial process [see Fig. 5(a)]. Comparing the calculated database on the above model, γ values of 0.4 and 0.2 seem to be suitable for the 5 and 19 ps data, respectively. Thus, the fast relaxation process should be considered to be the relaxation process of a number of the photoinduced monovalent dimers. However, even the spectral shape of reflectivity observed at 19 ps after photoexcitation is still different from that before the photoexcitation, corresponding to the formation of metastable state II observed in the time profile shown in Fig. 5(a). In addition, the recovery of this remnant part to the original thermal-equilibrium state takes more than 500 ps. Disappearance of the CS phase will induce lattice relaxation via dimer distortion mode leading to a metastable condensed state of the lattice-distorted monovalent dimer. We tentatively assign the origin of metastable state II to this lattice-distorted CS state. The slow relaxation process of this state may correspond to the lattice-valence coupled relaxation process to the original CS phase. For real assignment, dynamical probing of the local structural deformation in the 1–10 ps time-region is necessary.

VI. EXCITATION INTENSITY DEPENDENCE

Figure 7 shows the excitation intensity dependence of the time-profile of the photoinduced reflectivity change in the CS phase. Both the intensity of the photoresponse and the relaxation time increase with enhanced excitation intensity. Figures 8(a)–8(c) show the excitation intensity dependence of the reflectivity change at 0.5, 5, and 19 ps after photoexcitation at several temperatures. For the 0.5 ps after photoexcitation, the photoresponse shows a linear dependence on the excitation intensity below T_c, and $\Delta R/R$ increases with decreasing temperature from T_c. In contrast, the photoresponse observed at a long delay time shows different behavior. As shown in Fig. 8(c), the change in reflectivity at long delay times increases hyperlinearly as the intensity increases. This observed behavior suggests that the relaxation dynamics of the photoinduced state is governed by the density of the photoinduced state. Using fitting analysis, the excitation intensity dependence of the relaxation time of the fast relaxation process at various temperatures is plotted in Figs. 8(d)–8(f). The relaxation time typically increases as the pump intensity increases. The stability of the photoinduced state is enhanced with stronger excitation. In addition, the slope of the excitation intensity dependence of the relaxation time increases with increasing the sample temperature near T_c. Just after the photoirradiation, the Franck-Condon-type photoexcited state will spread into a finite-size "domain" of the photoinduced metastable state I with charge-transfer independently among dimers, consistent with the observed result that the data at 0.5 ps show a linear power dependence. As the density of the photoinduced metastable state I becomes larger, the stability of each domain is enhanced. ET_2X is well-known as a typical example of the photoeffect in CO systems[8] and similar excitation intensity dependence of the relaxation time was reported for ET_2X. In this case, the lifetime of the photoinduced state in $[\theta-(BEDT\text{-}TTF)_2RbZn(SCN)_4]$ increased with increasing pump intensity. Comparing the previously reported results with our results for $Et_2Me_2Sb[Pd(dmit)_2]_2$, it should be noted that PIPT dynamics seem to be common and universal for both systems though the phase transition mechanism is quite different. In addition to the CO system, similar charge-lattice coupled dynamics accompanied with coherent vibration have been observed for the PIPT process between the neutral (N) and ionic (I) phases in tetrathiafulvalene-chloranil (TTF-CA) crystals. It is an attractive problem for theoretical studies to propose a unified model for explanation of ultrafast charge-lattice coupled dynamics in molecule-based systems with different natures such as N-I, CO, and CS systems. Challenging trials for constructing a common theoretical framework which reproduce the photoinduced dynamics in these systems has been just started.[20,21]

VII. TEMPERATURE DEPENDENCE OF THE RELAXATION PROCESS

Figure 2(c) shows the temperature dependence of the relaxation time of the fast relaxation component (τ) derived from the fitting procedure. The relaxation time increases with warming up of the sample and appears to diverge at around T_c. This effect seems to correspond to the so-called "critical slowing down" phenomenon characteristic of the phase transition under thermoequilibrium conditions. According to the critical slowing down idea, the divergence of τ is explained by that of the correlation length of the fluctuation (ξ). The relation can be represented by the following equation, $\tau \propto \xi^z$ (z: dynamical exponent). In the case of the photoinduced effect, such a fluctuation will correspond to the size of the photoinduced metastable I domain directly generated by the photoexcitation. The present system shows the first order phase transition under a thermoequilibrium condition, and it raises a question whether the critical slowing down idea is appropriate for this case. However, at the present stage, we tentatively consider that this idea seems to be applicable for the photoinduced case as discussed below.

We have been able to estimate the ratio between $\Delta R/R$ and the static change in the reflectivity $\{[R(T)-R(T_c)]/R(T_c)\}$ based on the temperature dependence of the degree of the photoinduced $\Delta R/R$. When we assume a temperature-independent quantum yield for the generation of the photoinduced state, the above ratio should be proportional to the relative domain size of the photoinduced state ($\propto \xi^2$, when we assume a two-dimensional domain). The obtained result, which was normalized to the size of the photoinduced domain at 16.6 K, is plotted in Fig. 2(d). As the sample temperature approaches T_c, the domain size estimated from the reflectivity change increases and shows divergence corresponding to the divergence of the relaxation time of the photoinduced state. The observed parallel behavior of the ξ and τ strongly supports the idea that the concept of critical slowing down is valid in this case.

We tried to fit these data with the formula $\tau \propto |T-T_w|^{-\nu z}$ and $\xi \propto |T-T_w|^{-\nu}$, where ν is the critical exponent of ξ. The exponent of τ shows a small value ($\nu z = 0.46 \pm 0.15$, $T_w = 69.3 \pm 2.9$ K), and ν also shows a small value ($\nu = 0.11 \pm 0.06$) when two-dimensional domains are assumed. The deduced z is about 4. This value of z may be consistent with the typical value of the mean field approximation in the second-order phase transition systems in which the order parameter is the conserved value.[22] On the other hand, the value of 0.11 for ν is too small compared to theoretical work on the two-dimensional Ising spin model.[23] The discrepancy in the exponent may partly reflect the first order nature of the CS to DM transition in $Et_2Me_2Sb[Pd(dmit)_2]_2$ and require advanced theoretical investigation. It should be noted that this value is consistent with the previously reported value in the fast component of the relaxation of the photoinduced state in the two-dimensional CO system $\alpha-(BEDT\text{-}TTF)_2I_3$ ($\nu z = 0.3-0.65$) under weak photoexcitation.[8] The observed similarity in the exponent of τ may suggest universality in the initial relaxation of the photoinduced state of CS and CO systems.

VIII. SUMMARY

In summary, we have studied photoinduced reflectivity changes in the $Et_2Me_2Sb[Pd(dmit)_2]_2$ single crystal that shows the CS phase transition. Photoexcitation induced (1) a large and abrupt spectral change corresponding to the formation of metastable state I and subsequent, (2) fast relaxation of the metastable state I, and (3) formation of the metastable state II in the CS phase. The photoinduced dynamics, especially fast relaxation process, was independent of the excitation photon energy, i.e., selection of excited states. In other words, the photoinduced metastable state I is generated within 0.5 ps after photoexcitation irrespective of the initial Franck-Condon state. According to multilayer analysis, this metastable state I should be the averaged valence state similar to the high temperature DM state, then the CS state was melted by photoexcitation. The conversion efficiency is 4 to 5 dimers per 1 excitation photon at 0.5 ps after photoexcitation. The relaxation time of the subsequent fast relaxation shows excitation intensity and temperature dependence. With increasing excitation intensity, the relaxation time of the fast relaxation and the generated quantity of metastable state II increase. For the temperature dependence, the critical slowing down phenomenon has been observed in the fast relaxation process. Then, the relaxation dynamics of the photoinduced metastable state I is closely correlated with the coherence length of the fluctuation of the DM state. Since the conversion efficiency exceeds one and the photoinduced state is closely correlated with the fluctuation of the charge and lattice, we classify this photoinduced spectral change as PIPT.

ACKNOWLEDGMENTS

The authors thank T. Yamamoto for useful discussions. This work was partly supported by a Grant-in Aid for Scientific Research on Priority Areas (Grant No. 18028010), Grant-in-Aid for Creative Scientific Research (Grant No. 16GS0219) and G-COE program of JSPS.

*Present address: Department of Physics, Faculty of Science and Technology, Tokyo University of Science, Yamazaki 2641, Noda, Chiba 278-8510, Japan.

[1] For the review, K. Nasu, *Photo Induced Phase Transition* (World Scientific, Singapore, 2003).

[2] Y. Tokura, J. Phys. Soc. Jpn. **75**, 011001 (2006); E. Collet, M. Cointe, and H. Cailleau, J. Phys. Soc. Jpn. **75**, 011002 (2006); A. Cavalleri, M. Rini, and R. W. Schoenlein, J. Phys. Soc. Jpn. **75**, 011004 (2006); S. Koshihara and S. Adachi, *ibid.* **75**, 011005 (2006); D. J. Hilton, R. P. Prasankumar, S. A. Trugman, A. J. Taylor, and R. D. Averitt, *ibid.* **75**, 011006 (2006); S. Iwai and H. Okamoto, *ibid.* **75**, 011007 (2006), and references therein.

[3] M. Rini, R. Robey, N. Dean, J. Itatani, Y. Tomioka, Y. Tokura, R.

W. Schoenlein, and A. Cavalleri, Nature (London) **449**, 72 (2007).
[4] N. Tajima, J. Fujisawa, N. Naka, T. Ishihara, R. Kato, Y. Nishio, and K. Kajita, J. Phys. Soc. Jpn. **74**, 511 (2005).
[5] K. Yamamoto, S. Iwai, S. Boyko, A. Kashiwazaki, F. Hiramatsu, C. Okabe, N. Nishi, and K. Yakushi, J. Phys. Soc. Jpn. **77**, 074709 (2008).
[6] H. Okamoto, Y. Ishige, S. Tanaka, H. Kishida, S. Iwai, and Y. Tokura, Phys. Rev. B **70**, 165202 (2004).
[7] M. Chollet, L. Guerin, N. Uchida, S. Fukaya, H. Shimoda, T. Ishikawa, K. Matsuda, T. Hasegawa, A. Ota, H. Yamochi, G. Saito, R. Tazaki, S. Adachi, and S. Koshihara, Science **307**, 86 (2005).
[8] S. Iwai, K. Yamamoto, A. Kashiwazaki, F. Hiramatsu, H. Nakaya, Y. Kawakami, K. Yakushi, H. Okamoto, H. Mori, and Y. Nishio, Phys. Rev. Lett. **98**, 097402 (2007).
[9] R. Kato, Chem. Rev. (Washington, D.C.) **104**, 5319 (2004).
[10] R. Kato, Y. Kashimura, S. Aonuma, N. Hanasaki, and H. Tajima, Solid State Commun. **105**, 561 (1998).
[11] M. Tamura and R. Kato, J. Phys.: Condens. Matter **14**, L729 (2002).
[12] M. Tamura, K. Takenaka, H. Takagi, S. Sugai, A. Tajima, and R. Kato, Chem. Phys. Lett. **411**, 133 (2005).
[13] M. Tamura, A. Tajima, and R. Kato, Synth. Met. **152**, 397 (2005).
[14] Y. Nishio (private communication).
[15] A. Nakao and R. Kato, J. Phys. Soc. Jpn. **74**, 2754 (2005).
[16] M. Tamura and R. Kato, Chem. Phys. Lett. **387**, 448 (2004).
[17] For example, H. Seo, J. Merino, H. Yoshioka, and M. Ogata, J. Phys. Soc. Jpn. **75**, 051009 (2006).
[18] T. Ishikawa, N. Fukazawa, Y. Matsubara, R. Nakajima, K. Onda, Y. Okimoto, S. Koshihara, M. Tamura, R. Kato, M. Lorenc, and E. Collet, Phys. Status Solidi C **6**, 112 (2009).
[19] H. Okamoto, H. Matsuzaki, T. Wakabayashi, Y. Takahashi, and T. Hasegawa, Phys. Rev. Lett. **98**, 037401 (2007).
[20] K. Yonemitsu, J. Phys. Soc. Jpn. **73**, 2868 (2004); **73**, 2879 (2004); **73**, 2887 (2004).
[21] K. Yonemitsu and N. Maeshima, Phys. Rev. B **76**, 075105 (2007).
[22] J. Cardy, *Scaling and Renormalization in Statistical Physics* (Cambridge University Press, Cambridge, England, 1996).
[23] M. P. Nightingale and H. W. J. Blote, Phys. Rev. Lett. **76**, 4548 (1996).